

# Dynamics of water confined in single- and double-wall carbon nanotubes

E. Mamontov<sup>a)</sup>*NIST Center for Neutron Research, National Institute of Standards and Technology, Gaithersburg, Maryland 20899-8562 and Department of Materials Science and Engineering, University of Maryland, College Park, Maryland 20742-2115*

C. J. Burnham

*Department of Physics, The University of Houston, Houston, Texas 77204*

S.-H. Chen

*Department of Nuclear Science and Engineering, Massachusetts Institute of Technology, Cambridge, Massachusetts 02139*

A. P. Moravsky

*MER Corporation, Tucson, Arizona 85706*

C.-K. Loong, N. R. de Souza, and A. I. Kolesnikov

*Intense Pulsed Neutron Source Division, Argonne National Laboratory, Argonne, Illinois 60439*

(Received 8 December 2005; accepted 14 March 2006; published online 16 May 2006)

Using high-resolution quasielastic neutron scattering, we investigated the temperature dependence of single-particle dynamics of water confined in single- and double-wall carbon nanotubes with the inner diameters of  $14 \pm 1$  and  $16 \pm 3$  Å, respectively. The temperature dependence of the alpha relaxation time for water in the 14 Å nanotubes measured on cooling down from 260 to 190 K exhibits a crossover at 218 K from a Vogel-Fulcher-Tammann law behavior to an Arrhenius law behavior, indicating a fragile-to-strong dynamic transition in the confined water. This transition may be associated with a structural transition from a high-temperature, low-density ( $< 1.02$  g/cm<sup>3</sup>) liquid to a low-temperature, high-density ( $> 1.14$  g/cm<sup>3</sup>) liquid found in molecular dynamics simulation at about 200 K. However, no such dynamic transition in the investigated temperature range of 240–195 K was detected for water in the 16 Å nanotubes. In the latter case, the dynamics of water simply follows a Vogel-Fulcher-Tammann law. This suggests that the fragile-to-strong crossover for water in the 16 Å nanotubes may be shifted to a lower temperature. © 2006 American Institute of Physics. [DOI: [10.1063/1.2194020](https://doi.org/10.1063/1.2194020)]

## I. INTRODUCTION

Following the study by Hummer *et al.*,<sup>1</sup> who predicted pulselike transmission of water molecules through carbon nanotubes, numerous molecular dynamics (MD) simulation studies of the dynamics of water in carbon nanotubes were performed.<sup>2–11</sup> A lattice gas model was used to demonstrate that pulselike transmission of water molecules through a carbon nanotube is a generic liquid-state phenomenon that follows from simple stochastic rules.<sup>12</sup> However, the experimental measurements of the dynamics of water in nanotubes have lagged behind. Only recently an inelastic neutron scattering measurement probed the density of states and vibrational mean-square displacements of hydrogen atoms in water confined in carbon nanotubes with the inner diameter of 14 Å.<sup>13</sup> The experimental findings of extremely soft dynamics of water at low temperatures<sup>13</sup> were consistent with the MD model that predicted shell water molecules near the inner wall of the nanotubes plus central single-file water chain. The large mean-square displacement of hydrogen at temperatures down to 50 K could be explained by anomalously en-

hanced thermal motions in the water chain due to a low-barrier, flattened, highly anharmonic potential. In this work, we report the results of quasielastic neutron scattering (QENS) studies carried out with a very high-energy resolution ( $\mu$ eV) sufficient to probe translational diffusion of water molecules in carbon nanotubes. Water was confined in single-wall nanotubes (SWNTs) and double-wall nanotubes (DWNTs) with the inner diameters of 14 and 16 Å, respectively. The temperature dependence of the relaxation time for the confined water suggested the presence of fragile-to-strong dynamic transition in the SWNT in the temperature range of 260–190 K, but not in the DWNT in the temperature range of 240–195 K. The dynamic transition for water in the SWNT was possibly associated with a structural transition from bulklike confined water at higher temperatures to water forming a shell layer near the inner wall of the nanotubes plus water chain at lower temperatures.

## II. EXPERIMENT

The raw SWNT sample was produced by direct current arc vaporization of graphite-metal composite anodes. The metal component consisted of Co/Ni catalyst in a 3:1 mixture. The DWNT material was synthesized by chemical

<sup>a)</sup>Present address: SNS Project, Oak Ridge National Laboratory, Bldg. 8600, Oak Ridge, TN 37831-6475. Electronic mail: mamontove@ornl.gov

vapor deposition technique. The subsequent purification with hydrochloric acid was followed by the oxidation of non-tube carbon components in air at 300–600 °C. These preparation and purification steps produced micrometer-long nanotubes of a high purity, that is, with low metal catalyst content and low non-tube carbon content. The nanotube ends were opened by exposing the purified material to air at 420 °C for about 30 min. The samples were characterized by transmission electron microscopy (TEM) and small-angle neutron diffraction. For both the SWNT and DWNT, the (0,1) reflection of the two-dimensional (2D) hexagonal lattice of the bundle was evident in the diffraction data. The mean diameter of the SWNT was  $14 \pm 1$  Å, and the mean inner and outer diameters of the DWNT were  $16 \pm 3$  and  $23 \pm 3$  Å, respectively. The water absorption was controlled following identical protocols for all nanotube samples: a mixture of de-ionized water and the nanotube material was equilibrated for 2 h in an enclosed volume at 110 °C; excess water was then evaporated at 45 °C until reaching the targeted water mass fraction. In this work, 2.6 g of SWNT and 1.2 g of DWNT samples were loaded with 11 wt % of water each. Hydrated nanotubes were placed in thin annular aluminum sample holders chosen to ensure greater than 90% neutron beam transmission through the samples in order to minimize the effects due to multiple scattering. The sample holders were sealed with indium O-rings and mounted onto the cold stage of a closed-cycle refrigerator, the temperature of which was controlled within  $\pm 0.1$  K. QENS experiments were performed using the high flux backscattering spectrometer<sup>14</sup> (HFBS) at the National Institute of Standards and Technology (NIST) Center for Neutron Research. The incident neutron wavelength at the HFBS is varied via Doppler shifting about a nominal value of  $6.271$  Å ( $E_0=2.08$  meV). After scattering from the sample, only neutrons having a fixed final energy of 2.08 meV are measured by the detectors as ensured by Bragg reflection from analyzer crystals. The instrument was operated with a dynamic range of  $\pm 35$   $\mu$ eV, providing the energy resolution of 1.2  $\mu$ eV, full width at half maximum. The measurements were performed at the following temperatures: 260, 250, 240, 230, 220, 210, 200, 190, and 5 K for the SWNT, and 240, 225, 210, 195, and 5 K for the DWNT. The spectra obtained at 5 K were used as the resolution functions.

### III. RESULTS AND ANALYSIS

The data collected at  $Q=1.32$  Å<sup>-1</sup> are shown in Fig. 1 as a representative example. The QENS signal due to mobile water molecules is dominated by scattering from hydrogen atoms because of the large incoherent neutron scattering cross section of hydrogen. The width of the signal decreases as the temperature is decreased, indicating a slower motion. The spectra were analyzed using a model scattering function,  $S(Q, E)$ , that included an elastic term due to immobile atoms and a Lorentzian broadening term due to mobile hydrogen atoms,

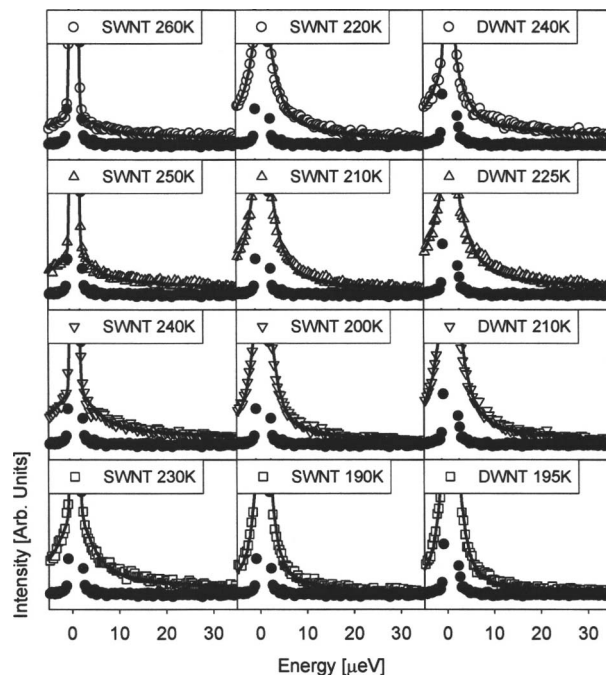


FIG. 1. QENS spectra of water in the SWNT and DWNT samples. Open symbols: the scattering intensities measured at  $Q=1.32$  Å<sup>-1</sup>. Filled symbols: the resolution function (5 K data) measured at the same  $Q$  value. The data are plotted using the same scaling of the ordinate axes at each temperature point. The energy range and elastic peaks are truncated to emphasize the QENS broadening.

$$S(Q, E) = x(Q)\delta(E) + [1 - x(Q)] \frac{1}{\pi} \frac{\Gamma(Q)}{E^2 + \Gamma(Q)^2} + BE + C, \quad (1)$$

convolved with the spectrometer resolution function. Here  $x(Q)$  is the fraction of the elastic scattering in the signal,  $\Gamma(Q)$  is the Lorentzian half width at half maximum (HWHM), and the linear term ( $BE+C$ ) describes the inelastic background. The  $Q$  dependence of the parameter  $\Gamma(Q)$  plotted in Figs. 2 and 3 shows that the QENS broadening increases with  $Q$  before reaching its limiting value. Such behavior is a fingerprint of a translational jump diffusion process with a distribution of jump length. Assuming a Gaussian distribution of jump lengths, we fit the QENS broadening with the expression<sup>15</sup>

$$\Gamma(Q) = \frac{\hbar}{\tau_{\text{res}}} [1 - \exp(-D_{\text{trans}} Q^2 \tau_{\text{res}})]. \quad (2)$$

Here  $\tau_{\text{res}}$  is a residence time between jumps, and the translational diffusion coefficient  $D_{\text{trans}} = \langle r^2 \rangle / 6\tau_{\text{res}}$ , where  $\langle r^2 \rangle$  is the mean-squared diffusion jump length. The values of  $\tau_{\text{res}}$ ,  $D_{\text{trans}}$ , and mean jump length obtained from the fitting are shown in Table I. The values of the diffusion coefficients appear to be close to those obtained for supercooled bulk water at comparable temperatures.<sup>16,17</sup> This is rather unexpected, because the effect of confinement usually leads to a decrease of diffusion coefficient compared to bulk water. On the one hand, the surface of carbon nanotubes is hydrophobic, unlike hydrophilic pore surfaces in typical confining matrices (silicas). Together with a reduced number of hydrogen bonds per water molecule, this may result in higher diffusion coefficients compared to those measured in typical confining

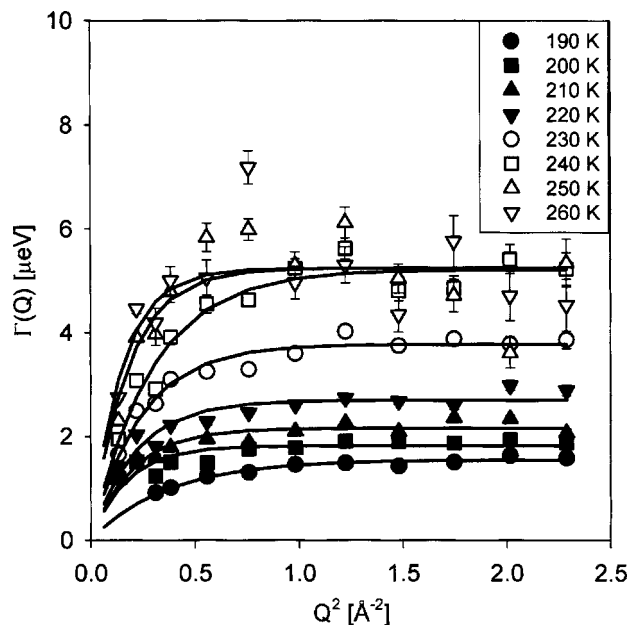


FIG. 2. The  $Q$  dependence of the HWHM of the Lorentzian QENS broadening for water in the SWNT fitted with Eq. (2).

matrices and counterbalance the geometrical effects of confinement in nanotubes. On the other hand, it is possible that our analysis of QENS data overestimates the diffusion coefficients. For a translational diffusion process, the low- $Q$  data broadening, which defines the diffusion coefficient, is proportional to  $D_{\text{trans}}Q^2$  and characterized by smaller quasielastic broadening. Besides, these data have to be measured at the low-angle detectors of the backscattering spectrometer, which have somewhat worse energy resolution compared to the rest of the detectors.<sup>14</sup> As a result, the spectrometer may be unable to capture the entire range of diffusivities, thus missing a slower fraction and yielding an artificially enlarged

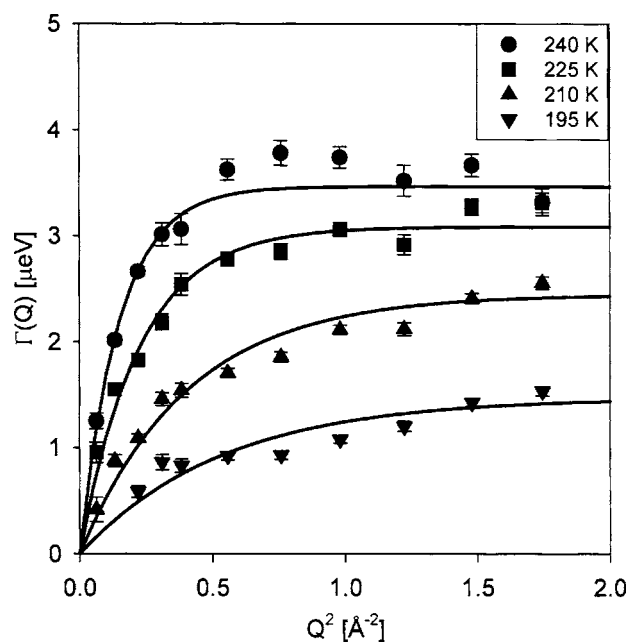


FIG. 3. The  $Q$  dependence of the HWHM of the Lorentzian QENS broadening for water in the DWNT fitted with Eq. (2).

TABLE I. Residence times and translational diffusion coefficients obtained from fitting the HWHM of the Lorentzian QENS broadening with Eq. (2). The mean jump length was calculated from the fit parameters  $\tau_{\text{res}}$  and  $D_{\text{trans}}$  as  $(\langle r^2 \rangle)^{1/2} = (6\tau_{\text{res}}D_{\text{trans}})^{1/2}$ . Standard deviation values are shown in parentheses.

$T$ (K)	$\tau_{\text{res}}$ ( $\times 10^{-12}$ s)	$D_{\text{trans}}$ ( $\times 10^{-10}$ m <sup>2</sup> /s)	$(\langle r^2 \rangle)^{1/2}$ (Å)
Single-wall nanotubes			
260	125 (7)	5.4 (1.9)	6.4 (0.9)
250	125 (7)	4.6 (1.4)	5.8 (0.7)
240	126 (3)	2.7 (0.3)	4.5 (0.2)
230	174 (3)	2.4 (0.2)	5.0 (0.2)
220	243 (7)	1.9 (0.3)	5.3 (0.3)
210	304 (8)	1.7 (0.2)	5.5 (0.3)
200	361 (13)	1.6 (0.3)	5.9 (0.5)
190	423 (7)	0.7 (0.1)	4.1 (0.2)
Double-wall nanotubes			
240	190 (6)	3.5 (0.7)	6.4 (0.5)
225	213 (4)	2.1 (0.2)	5.2 (0.2)
210	268 (8)	0.9 (0.1)	3.9 (0.2)
195	445 (26)	0.4 (0.1)	3.3 (0.3)

effective diffusion coefficient. In fact, the values of the mean jump length listed in Table I are larger than those expected based on the density of water ( $\approx 3$  Å), suggesting that the values of the diffusion coefficient determined from the QENS data may be overestimated. Because the overestimate of the diffusion coefficient (and, therefore, mean jump length) is likely temperature dependent, the true temperature dependence of these parameters is difficult to assess. Fortunately, the reliability of the residence time values listed in Table I is much higher because they are determined from the high- $Q$  data, where the QENS broadening reaches its maximum for a translational diffusion process, and the energy resolution at the higher-angle detectors of the backscattering spectrometer is the best. Thus, the assessment of the residence times obtained from fitting the QENS broadening with Eq. (2) is much more accurate.

The temperature dependence of  $\tau_{\text{res}}$  is plotted in Fig. 4. For the DWNT, the latter can be well fitted with a Vogel-Fulcher-Tammann (VFT) law,  $\tau = \tau_0 \exp(DT_0/(T-T_0))$ ,  $T_0 = 172 \pm 1$  K, through the entire temperature range of the measurement. For the SWNT, the data obtained at the lowest-temperature points of 190, 200, and 210 K clearly demonstrate an Arrhenius temperature dependence with an activation energy of 5.4 kJ/mol (1.29 kcal/mol). This is about 2.5 times smaller compared to the effective activation energy (3.2 kcal/mol) of breaking a hydrogen bond at 258 K obtained from inelastic neutron scattering data on stretching vibrational band of supercooled water<sup>18</sup> and 3.8 times smaller than the activation energy for water in MCM-41-S silica with 14 Å diameter pores.<sup>19</sup> The Arrhenius-type dependence does not extrapolate into the higher-temperature region. Fitting the rest of the points with a VFT law yields the glass transition temperature  $T_0 = 203 \pm 12$  K. The crossover between the VFT and Arrhenius fits that occurs at 218 K shows a fragile-to-strong dynamic transition in confined water. Such a transition predicted for supercooled bulk water several years ago<sup>20</sup> was recently observed using QENS in

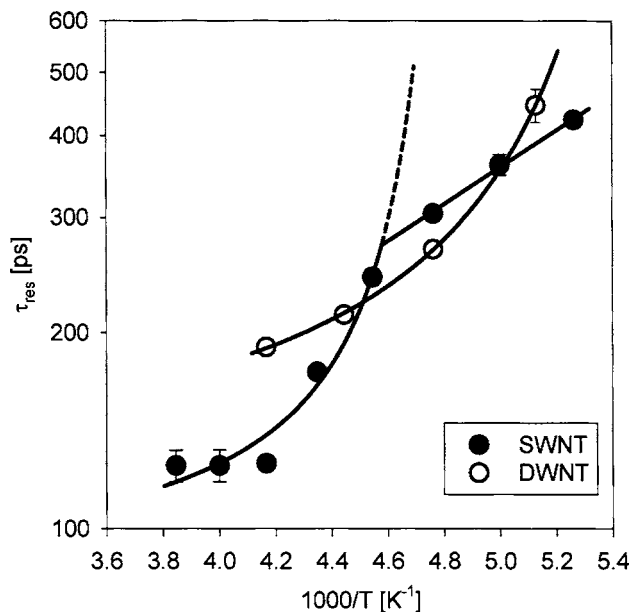


FIG. 4. The temperature dependence of the residence time and its fits for (1) water in the SWNT (filled points): a VFT law,  $\tau = \tau_0 \exp(DT_0/(T-T_0))$ ,  $T_0 = 203$  K above and an Arrhenius law,  $\tau = \tau_0 \exp(E_A/RT)$ , below the cross-over at 218 K; (2) water in the DWNT (open points): a VFT law,  $\tau = \tau_0 \exp(DT_0/(T-T_0))$ ,  $T_0 = 172$  K. Dashed line shows the extrapolation of the VFT fit for the SWNT into the lower-temperature region.

water confined in nanoporous silicas<sup>19,21</sup> at  $\approx 225$  K (ambient pressure) and surface water on CeO<sub>2</sub> nanoparticles<sup>22</sup> at  $\approx 215$  K. The origin of this transition is thought to be linked to a structural change in the liquid state.<sup>21</sup>

#### IV. DISCUSSION

A structural transition for water in (10,10) SWNT was observed at about 200 K in recent MD simulations.<sup>23</sup> The simulations were performed on a rigid (10,10) SWNT of 13.8 Å in diameter and 40 Å in length enclosing 126 water molecules. The water-carbon and water-water interactions were represented by a Lennard-Jones<sup>24</sup> and the TTM2-F water model of Burnham and Xantheas,<sup>25</sup> respectively. Using smeared charges and dipoles to model short-range electrostatic interactions, the TTM2-F polarizable flexible water model was able to accurately account for the high-level electronic structure data of water clusters and to reproduce the bulk behavior of ice and ambient liquid water. The Ewald sum for the long-range Coulomb interactions and standard boundary conditions were used. These simulations were performed using a “parallel tempering” molecular dynamics (PTMD) algorithm. The PTMD algorithm<sup>26</sup> calculates multiple simultaneous trajectories for the system, where each trajectory is assigned a different temperature, and the occasional swapping of temperatures between neighboring trajectories is employed in accordance with detailed balance under the Boltzmann distribution. PTMD can easily locate low-lying minima, as the temperature changes in the course of the simulation allow for escape over intermediate barriers when the system heats up and for annealing in the vicinity of low-energy regions of the potential energy surface when the system cools down. Figure 5 shows the structure of water in SWNT at low ( $T=150$  K) and high ( $T=250$  K) temperatures

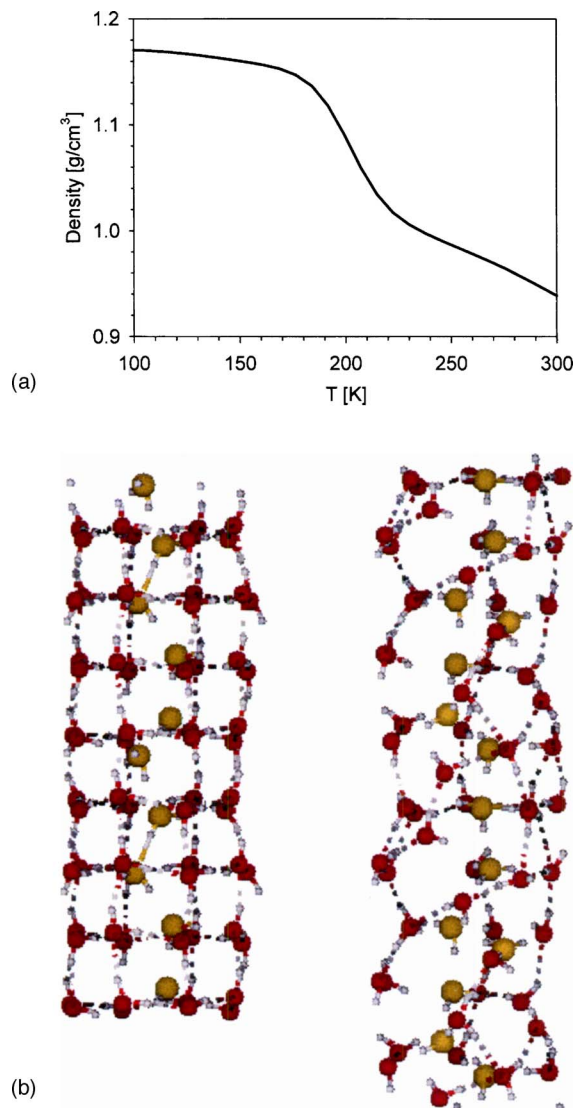


FIG. 5. (Color online) (a) The temperature dependence of the density of water in SWNT of 13.8 Å diameter as obtained from MD simulations (Ref. 23) showing a transition from low-density liquid to high-density liquid on cooling. (b) Structure of water confined inside a nanotube (Ref. 23). Below the phase transition ( $T=150$  K, left) the water molecules adopt a shell-chain geometry. The chain water molecules near the central tube axis are shown in yellow (lighter color). Above the phase transition ( $T=250$  K, right) the structure becomes a disordered H-bonded network similar to bulk water. Molecules within 2.5 Å of the central tube axis are colored yellow (lighter color), even though they are not structurally different from the rest of the molecules.

and temperature dependence of the water density obtained in PTMD simulations. The water density was calculated assuming that water occupies a cylinder with a diameter obtained from external zero position in the calculated radial distribution function of water across the SWNT. Almost all of the density change results from expansion along the cylinder axis. The radial change was small, about 0.15 Å over the whole temperature range. In contrast to bulk water, the high-temperature phase has lower density compared to the low-temperature phase. At temperatures below the transition the water molecules adopt a shell-chain geometry, whereas above the transition the structure becomes a disordered H-bonded network similar to bulk water. As far as the transition temperature is concerned, for the system of water mol-

ecules confined between two smooth hydrophobic plates separated by 11.0 Å, recent MD simulations<sup>27</sup> predict a shift of the overall phase diagram, including fragile-to-strong transition, to the temperatures lower by  $\approx 40$  K relative to bulk water. In our systems of water molecules confined in hydrophobic carbon nanotubes, the fragile-to-strong transition takes place, but the shift of its transition temperature is not observed for the SWNT with the inner diameter of 14 Å. Instead, the transition in the SWNT takes place at the temperature similar to the transition temperatures previously found for water in silicas.<sup>19,21</sup> However, for the DWNT with the inner diameter of 16 Å, such a shift of the fragile-to-strong transition to lower temperatures seems plausible since one can expect the VFT behavior observed in the temperature region of 240–195 K to switch eventually to an Arrhenius behavior at lower temperatures. Thus, in the future studies the MD predictions<sup>27</sup> should be tested on the DWNT at lower temperatures.

Even though the diffusion coefficients listed in Table I are not low [for instance,  $D_{\text{trans}}(298 \text{ K}) = 22.99 \times 10^{-10} \text{ m}^2/\text{s}$  in bulk water<sup>28</sup>], they are still much lower compared to the values predicted for central water chains in carbon nanotubes with the diameters ranging from 8.2 to 13.6 Å (Refs. 3 and 4). For example, for (10,10) nanotubes with the diameter of 13.6 Å, a diffusion coefficient of  $31 \times 10^{-10} \text{ m}^2/\text{s}$  ( $38 \times 10^{-10} \text{ m}^2/\text{s}$  along the nanotube axis and  $27 \times 10^{-10} \text{ m}^2/\text{s}$  in the perpendicular plane) was calculated at 298 K.<sup>3,4</sup> Also the residence times between jumps listed in Table I exceed the values predicted for the chain water in MD simulations<sup>1</sup> and continuous-time random walk calculations.<sup>29</sup> Therefore, the water dynamics probed in our experiment at low temperature is likely to be associated with the water molecules forming a shell layer near the inner wall of the nanotubes. On the other hand, because of the reduced number of hydrogen bonds and associated high mobility of the water molecules forming the central chain, their dynamics is probably too fast to contribute to the QENS signal on the assessable time scale of hundreds of picoseconds. In fact, in the presence of the shell water molecules the dynamics of the water chains must be rather difficult to observe because of the small ratio of the water molecules constituting the chains to the shell water molecules, such as 1:8 for the 14 Å SWNT, according to MD simulations<sup>13</sup> (for the 16 Å DWNT, the confined water structure comprises two hydrogen-bonded water shells). In order to assess the dynamics of the water chains, one has to either perform an experiment at lower temperatures, where the mobility of the shell water likely becomes too slow for the instrument resolution and thus contributes to the elastic signal, or use carbon nanotubes with the diameter small enough to prevent formation of the shell water layer. For the chain water, one can expect the molecular motion to resemble a single-file one-dimensional diffusion process, when the molecules cannot pass one another. The model scattering function for such a process, which would be different from the one for a regular diffusion process that we used in this work, is discussed in detail in Ref. 30.

We need to discuss the assumptions made when using Eqs. (1) and (2). Using the model scattering function in the

form of Eq. (1) implies that the dynamics of confined water assessable in the dynamic range of the spectrometer can be considered approximately a Debye type. This is because a Lorentzian broadening of the scattering function in the energy space corresponds to an exponential decay of the relaxation function in the time space. Non-Debye dynamics can be often represented by a stretched exponential relaxation function in the time space,  $\exp[-(t/\tau)^\beta]$ , with the stretch factor  $\beta \leq 1$  (whereas for the Debye-type dynamics  $\beta = 1$ ). Experiments on supercooled water confined in various nanoporous silicas<sup>31</sup> yielded low values of  $\beta \approx 0.5$ , indicating a strongly nonexponential relaxation function. On the other hand, almost Debye-type relaxation functions characterized by the stretch factors exceeding 0.8–0.9 were obtained for supercooled water on the surface of  $\text{ZrO}_2$  and  $\text{CeO}_2$  nanoparticles,<sup>22,32</sup> possibly due to less variations in the local molecular environment in the surface water. In this aspect, shell water on the inner surface of the nanotubes may bear more resemblance to surface water on nanoparticles. Additionally, a hydrophobic character of the surface-water interactions in carbon nanotubes may be expected to preclude a separation of water into the groups of molecules that interact with the hydrophilic surface and those that interact only with other water molecules. Such a separation likely contributes to the variations of local environments for water molecules near hydrophilic surface (for example, in oxides) leading to further stretching of the relaxation function, which should not occur for water in carbon nanotubes. Thus, our assumption of an exponential relaxation function may be reasonable. Using Eq. (2) implies that only the translational diffusion component contributes to the QENS broadening, whereas the rotational diffusion component is too fast for the dynamic range of the experiment. This is probably a reasonable assumption based on the computed average lifetime of a hydrogen bond of 5.6 ps for water in carbon nanotubes<sup>1</sup> that sets the time scale for the rotational diffusion component, which is well beyond the dynamic range of the HFBS.

## V. CONCLUSION

In summary, we have performed an approximate analysis of high-resolution incoherent quasielastic neutron scattering spectra of water confined within single- and double-wall carbon nanotubes using a simple jump diffusion model. We extract the temperature dependence of the residence time from the model, which we interpret to be approximately equivalent to the alpha relaxation time of the confined water. For water in the SWNT with an inner diameter of 14 Å, the relaxation time exhibits a crossover from a VFT law behavior to an Arrhenius law behavior, on cooling down, at  $\approx 218$  K. This temperature is close to the fragile-to-strong transition temperature, 225 K, previously found in systems with a hydrophilic surface. On the other hand, for water in the DWNT with the inner diameter of 16 Å, the relaxation time obeys a VFT law at least down to 195 K, leaving open a possibility that the fragile-to-strong transition is shifted to a lower temperature, as was recently predicted for the systems with hydrophobic surface-water interactions.<sup>27</sup>

## ACKNOWLEDGMENTS

The authors are thankful to D. Neumann and V. Garcia Sakai for critical reading of the manuscript. Utilization of the DAVE package<sup>33</sup> for the data analysis is acknowledged. This work utilized NIST neutron facilities supported in part by the National Science Foundation under Agreement No. DMR-0086210. The work performed at the Intense Pulsed Neutron Source was supported by the Office of Basic Energy Sciences, Division of Materials Science, U.S. Department of Energy under Contract No. W-31-109-ENG-38. One of the authors (C.J.B.) is thankful for a Grant from Argonne Theory Institute for his stay at the IPNS. The MD calculations were performed with a grant of time on the Argonne National Laboratory Jazz computer. C. J. B. is also thankful for the support by the Department of Energy, Office of Basic Energy Sciences under Contract No. DE-FG02-03ER46078.

- <sup>1</sup>G. Hummer, J. C. Rasaiah, and J. P. Noworyta, *Nature (London)* **414**, 188 (2001).
- <sup>2</sup>J. Marti and M. C. Gordillo, *Phys. Rev. B* **63**, 165430 (2001).
- <sup>3</sup>J. Marti and M. C. Gordillo, *Phys. Rev. E* **64**, 021504 (2001).
- <sup>4</sup>J. Marti and M. C. Gordillo, *J. Chem. Phys.* **114**, 10486 (2001).
- <sup>5</sup>K. Koga, G. T. Gao, H. Tanaka, and X. C. Zeng, *Nature (London)* **412**, 802 (2001).
- <sup>6</sup>W. H. Noon, K. D. Ausman, R. E. Smalley, and J. P. Ma, *Chem. Phys. Lett.* **355**, 445 (2002).
- <sup>7</sup>R. J. Mashl, S. Joseph, N. R. Aluru, and E. Jakobsson, *Nano Lett.* **3**, 589 (2003).
- <sup>8</sup>C. Dellago, M. N. Naor, and G. Hummer, *Phys. Rev. Lett.* **90**, 105902 (2003).
- <sup>9</sup>D. J. Mann and M. D. Halls, *Phys. Rev. Lett.* **90**, 195503 (2003).
- <sup>10</sup>F. Zhu and K. Schulten, *Biophys. J.* **85**, 236 (2003).
- <sup>11</sup>S. Sriraman, I. G. Kevrekidis, and G. Hummer, *Phys. Rev. Lett.* **95**, 130603 (2005).
- <sup>12</sup>L. Maibaum and D. Chandler, *J. Phys. Chem. B* **107**, 1189 (2003).
- <sup>13</sup>A. I. Kolesnikov, J.-M. Zanotti, C.-K. Loong, P. Thiyagarajan, A. P. Moravsky, R. O. Loutfy, and C. J. Burnham, *Phys. Rev. Lett.* **93**, 035503 (2004).
- <sup>14</sup>A. Meyer, R. M. Dimeo, P. M. Gehring, and D. A. Neumann, *Rev. Sci. Instrum.* **74**, 2759 (2003).
- <sup>15</sup>P. L. Hall and D. K. Ross, *Mol. Phys.* **42**, 673 (1981).
- <sup>16</sup>F. X. Prielmeier, E. W. Lang, R. J. Speedy, and H.-D. Lüdemann, *Phys. Rev. Lett.* **59**, 1128 (1987).
- <sup>17</sup>F. X. Prielmeier, E. W. Lang, R. J. Speedy, and H.-D. Lüdemann, *Ber. Bunsenges. Phys. Chem.* **92**, 1111 (1988).
- <sup>18</sup>M. A. Ricci and S.-H. Chen, *Phys. Rev. A* **34**, 1714 (1986).
- <sup>19</sup>L. Liu, S.-H. Chen, A. Faraone, C.-W. Yen, and C.-Y. Mou, *Phys. Rev. Lett.* **95**, 117802 (2005).
- <sup>20</sup>K. Ito, C. T. Moynihan, and C. A. Angell, *Nature (London)* **398**, 492 (1999).
- <sup>21</sup>A. Faraone, L. Liu, C.-Y. Mou, C.-W. Yen, and S.-H. Chen, *J. Chem. Phys.* **121**, 10843 (2004).
- <sup>22</sup>E. Mamontov, *J. Chem. Phys.* **123**, 171101 (2005).
- <sup>23</sup>C. J. Burnham *et al.* (unpublished).
- <sup>24</sup>J. H. Walther, R. Jaffe, T. Halicioglu, and P. Koumoutsakos, *J. Phys. Chem. B* **105**, 9980 (2001).
- <sup>25</sup>C. J. Burnham, J.-C. Li, S. S. Xantheas, and M. Leslie, *J. Chem. Phys.* **110**, 4566 (1999); C. J. Burnham and S.S. Xantheas, *ibid.* **116**, 1479 (2002); S. S. Xantheas, C. J. Burnham, and R. J. Harrison, *ibid.* **116**, 1493 (2002); C. J. Burnham and S. S. Xantheas, *ibid.* **116**, 1500 (2002); **116**, 5115 (2002).
- <sup>26</sup>For example, D. J. Earl and M. W. Deem, *J. Phys. Chem. B* **108**, 6844 (2004).
- <sup>27</sup>P. Kumar, S. V. Buldyrev, F. W. Starr, N. Giovambattista, and H. E. Stanley, *Phys. Rev. E* **72**, 051503 (2005).
- <sup>28</sup>R. Mills, *J. Phys. Chem.* **77**, 685 (1973).
- <sup>29</sup>A. Berezhkovskii and G. Hummer, *Phys. Rev. Lett.* **89**, 064503 (2002).
- <sup>30</sup>K. Hahn, H. Jobic, and J. Karger, *Phys. Rev. E* **59**, 6662 (1999).
- <sup>31</sup>L. Liu, A. Faraone, C.-Y. Mou, C.-W. Yen, and S.-H. Chen, *J. Phys.: Condens. Matter* **16**, S5403 (2004).
- <sup>32</sup>E. Mamontov, *J. Chem. Phys.* **123**, 024706 (2005).
- <sup>33</sup><http://www.ncnr.nist.gov/dave>